Attenuation of Interference in EEG Signals using the Adaptive Recursive Least Squares Algorithm

Manoel R. Caetano Junior and Rafael Ferrari

***Abstract*— In SSVEP-based BCIs, commands are generated by detecting oscillatory patterns in EEG signals. However, when these signals are affected by significantly interference, the identification task becomes more complex. To address this, we propose a novel spatio-temporal filtering technique called M-RLS-CCA, a modified version of the RLS-CCA method. We evaluated its performance against RLS-CCA and standalone spatial filtering using CCA. We also investigated whether signals from non-occipital regions can provide information about interference in occipital signals, helping to reduce such interference. To assess the method across different electrode configurations, accuracy and ITR were used as metrics. Results show that both M-RLS-CCA and RLS-CCA outperform spatial filtering with CCA alone, regardless of electrode setup. Moreover, M-RLS-CCA showed a slight improvement compared to the original approach.**

***Keywords*— Adaptive Filtering, Brain-Computer Interface, Steady-State Visually Evoked Potentials, Recursive Least Squares**

I. Introduction

A brain-computer interface (BCI), or brain-machine interface (BMI), enables communication between the brain and a computational system by processing electrical brain activity [1]. By decoding brain signals, the BCI system generates commands to control external devices, bypassing conventional motor pathways like muscles and peripheral nerves. This alternative channel is used in applications such as assistive technologies, electronic games, and rehabilitation [2].

In BCI systems, electroencephalography (EEG) is widely used as the primary method for recording brain electrical activity. As a noninvasive technique that uses electrodes placed on the scalp, EEG offers advantages such as ease of use, portability, and low cost, making it the preferred choice in most BCI applications. However, it suffers from inferior signal quality with reduced signal-to-noise ratio (SNR) compared to invasive methods [3].

In recent years, the steady-state visually evoked potentials (SSVEP) paradigm has gained attention due to its high information transfer rate (ITR) and minimal user training [4]. An SSVEP-based BCI presents flickering stimuli at different frequencies, with each frequency linked to a command. The user selects a command by focusing on the corresponding stimulus. Neurons in the visual cortex synchronize their electrical activity with the flickering frequency, producing evoked potentials that exhibit sinusoidal characteristics at the fundamental and harmonic frequencies [5].

Manoel R. Caetano Junior, DCA-FEEC, UNICAMP, e-mail: m240652@dac.unicamp.br; Rafael Ferrari, DCA-FEEC, UNICAMP, e-mail: rafaelf@unicamp.br. This study was financed in part by the Coordenação de Aperfeiçoamento de Pessoal de Nível Superior – Brasil (CAPES) – Finance Code 001, and by the PROGRAMA DE INCENTIVO A NOVOS DOCENTES (PIND) - UNICAMP.

Evoked potential detection has traditionally used power spectral density analysis (PSDA) [6], [2], though recent studies have shown time-domain techniques to be more effective. One of the most widely used approaches is canonical correlation analysis (CCA), originally proposed by Lin et al. [7]. This spatial filtering technique enhances classification by increasing the SNR of evoked potentials. Filter Bank Canonical Correlation Analysis (FBCCA) further improves performance by combining CCA with a filter bank [4]. Recently, Wang et al. [8] proposed a combination of the CCA with an adaptive signal enhancement filtering using recursive least squares (RLS-CCA) to reduce interference in signals from occipital lobe electrodes, outperforming classification with standard CCA.

The main objective of this work is to propose a modification to the filtering technique of the RLS-CCA method, which we call M-RLS-CCA, with the aim of improving the detection of evoked potentials. This proposal constitutes the primary contribution of the present study. Additionally, another point of interest is to investigate whether different regions of the cerebral cortex can provide reference signals that help improve the SNR of signals recorded in the occipital region. To answer these questions, the performance of each of the systems will be evaluated based on two main criteria: accuracy and information transfer rate (ITR).

This paper is organized as follows. Section II presents the problem of adaptive filtering in SSVEP-based BCI, as well as the original filtering approach using the RLS algorithm [8]. Section III presents the modified filtering method proposed in this work. Section IV details the experimental methodology. Section V presents the performance comparisons of the methods. Finally, Section VI concludes the paper.

II. Problem Definition

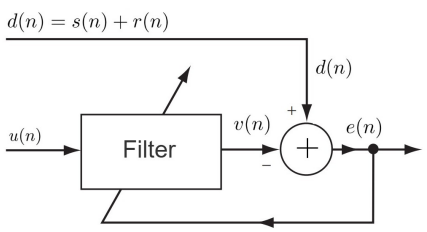

Fig. 1. Block diagram illustrating the signal enhancement problem.

Figure 1 presents a schematic illustration of the signal enhancement problem [9]. In the classical approach, two main signals are used: the primary signal, denoted by $d(n)$, which contains the desired signal $s(n)$ corrupted by the interference $r(n)$; and the reference signal, denoted by $u(n)$. It is assumed

that: (i) $s(n)$ and $r(n)$ are uncorrelated; (ii) $s(n)$ and $u(n)$ are uncorrelated; and (iii) $r(n)$ and $u(n)$ are correlated. The goal of the filtering process is to use the reference signal $u(n)$ to estimate the interference component $r(n)$, and then subtract it from the reference signal in order to estimate $s(n)$.

For each sample at time n, the filter generates a response $v(n)$, which is compared with $d(n)$, producing an error signal, $e(n) = d(n) - v(n)$, that is used to adjust the filter parameters.

A commonly used metric to adjust filter parameters is the minimization of the mean squared error (MSE) between the primary signal and the filter's output.

If the assumptions (i), (ii) and (iii) hold, the minimum MSE leads to an error signal that corresponds to an estimate of the desired signal $s(n)$ [9].

In the context of SSVEP BCI [8], $d(n)$ represents the signal recorded by an electrode in the occipital lobe, $s(n)$ is the visually evoked potential and $r(n)$ is an interference. $u(n)$, on the other hand, is a signal from a set of electrodes that contains information about $r(n)$ but do not register the evoked potential. In this scenario, it is assumed that most of the energy associated with the evoked potentials is located in the occipital lobe [10], [4] while electrodes from other regions capture little to none of these potentials. When applying the filtering process, the best scenario occurs when all interference is canceled out ($v(n) = r(n)$), and in this case, $e(n) = s(n)$, i.e., the error signal represents the evoked potentials.

In the original work, Wang et al. [8] proposed using the average signal collected from a set of electrodes located outside the occipital lobe as a reference signal. In this case, the reference is denoted by $\bar{u}(n)$, as illustrated in Figure 2. The structure that models the filter is a linear finite impulse response (FIR) filter. This filter is characterized by a coefficient vector $\mathbf{w}(n)$, which defines the filter's tap weights. The filter performs a convolution operation between the input signal $\bar{u}(n)$ and the coefficient vector $\mathbf{w}(n) = [w_0(n), w_1(n), \ldots, w_{N-1}(n)]$, where N is the number of tap weights in the filter. To perform this convolution, the input sample vector is defined as

$$\bar{\mathbf{u}}(n) = [\bar{u}(n),\ \bar{u}(n-1),\ \ldots,\ \bar{u}(n-N+1)]^T \qquad (1)$$

Then, the output at a given time instant n is

$$v(n) = \sum_{j=0}^{N-1} w_j(n) \cdot \bar{u}(n-j) = \mathbf{w}^T(n) \cdot \bar{\mathbf{u}}(n) \qquad (2)$$

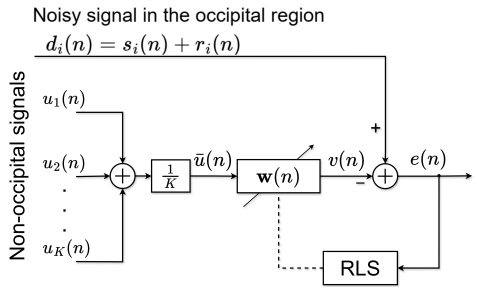

Fig. 2. Block diagram describing the filtering of an occipital signal using the average of non-occipital signals as the reference input.

The RLS algorithm [9] is used to update the weight vector at each iteration n.

The process illustrated in Figure 2 is applied to each i-th occipital signal $d_i(n)$ used in the classification process. After filtering, the error signals, which are estimates of the evoked potentials present in the occipital signals, are used as inputs to the CCA, where spatial filtering and subsequent classification occur. The combination of temporal filtering using RLS together with spatial filtering via CCA is referred to as the RLS-CCA technique [8]. The spatial filtering and classification process using CCA will be described in Subsection IV-A.

III. M-RLS-CCA

Our proposal consists of a generalization of the filtering technique presented in [8] and discussed in Section II. The main modification lies in the application of an individual FIR filter for each reference signal $u_i(n)$. With this approach, the RLS algorithm is used to simultaneously adjust the coefficients of all filters at each iteration n, as illustrated in Figure 3. The main advantage of this method is that, if a reference signal does not significantly contribute to minimizing the error signal, which leads to the estimation of the desired signal $s(n)$, the weights of the filter associated with that signal can be reduced, thus decreasing its influence on the estimation of the interferences present in the occipital signals. In contrast, when averaging the reference signals, all of them contribute equally to the estimation, including those that do not carry relevant information about the interferences or have poor SNR.

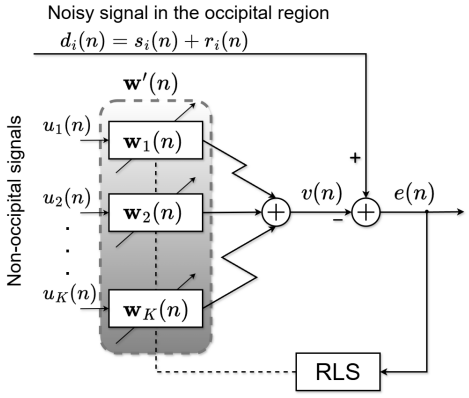

Fig. 3. Block diagram illustrating the filtering of an occipital signal using multiple FIR filters, one filter for each reference signal.

To enable the simultaneous adaptation of all filters using the RLS algorithm, it is necessary to slightly modify the input signals. Specifically, to accommodate K different signals, we define the the vector $\mathbf{u}'(n) \in \mathbb{R}^{KN\times 1}$ as

$$\mathbf{u}'(n) = \left[\mathbf{u}_1(n)^T,\ \mathbf{u}_2(n)^T,\ \ldots,\ \mathbf{u}_K(n)^T\right]^T, \qquad (3)$$

where each input vector $\mathbf{u}_i(n) = [u_i(n), \ldots,\ u_i(n-N+1)]^T$ corresponds to the i-th reference signal.

Similarly, the filter coefficient vector $\mathbf{w}'(n) \in \mathbb{R}^{KN\times 1}$, is defined as

$$\mathbf{w}'(n) = \left[\mathbf{w}_1(n)^T,\ \mathbf{w}_2(n)^T,\ \ldots,\ \mathbf{w}_K(n)^T\right]^T, \qquad (4)$$

where $\mathbf{w}_i(n) = [w_{i,0}(n), \ldots, w_{i,N-1}]^T$ is the filter associated with the i-th reference signal.

The filter output at iteration n is then computed as

$$v(n) = \mathbf{w'}^T(n)\,\mathbf{u'}(n). \tag{5}$$

After filtering, the resulting estimates of the occipital signals, $e(n)$, are fed into the CCA, as done in the original RLS-CCA method. Since there is one filter for each reference signal, we refer to this method as Multi-Filter RLS-CCA (M-RLS-CCA).

IV. Methodology

A. Canonical Correlation Analysis

Canonical Correlation Analysis is a multivariate statistical technique used to measure the underlying correlation between two multidimensional variables [7].

Considering two multidimensional variables $\mathbf{X}$ and $\mathbf{Y}$, and their linear combinations $\mathbf{x} = \mathbf{X}^\top \mathbf{z}_x$ and $\mathbf{y} = \mathbf{Y}^\top \mathbf{z}_y$, the technique aims to find vectors $\mathbf{z}_x$ and $\mathbf{z}_y$ that define projection directions for $\mathbf{X}$ and $\mathbf{Y}$, respectively, such that the resulting canonical variables $\mathbf{x}$ and $\mathbf{y}$ exhibit maximum correlation. To determine the weight vectors, it is necessary to solve the following optimization problem

$$\max_{\mathbf{z}_x, \mathbf{z}_y} \rho(\mathbf{x}, \mathbf{y}) = \frac{\mathbf{z}_x^\top E\{\mathbf{X}\mathbf{Y}^\top\}\mathbf{z}_y}{\sqrt{\mathbf{z}_x^\top E\{\mathbf{X}\mathbf{X}^\top\}\mathbf{z}_x} \cdot \sqrt{\mathbf{z}_y^\top E\{\mathbf{Y}\mathbf{Y}^\top\}\mathbf{z}_y}} \tag{6}$$

where $E\{\mathbf{X}\mathbf{Y}^\top\}$ is the cross-covariance matrix between $\mathbf{X}$ and $\mathbf{Y}$, $E\{\mathbf{X}\mathbf{X}^\top\}$ is the autocovariance matrix of $\mathbf{X}$, and $E\{\mathbf{Y}\mathbf{Y}^\top\}$ is the autocovariance matrix of $\mathbf{Y}$.

In SSVEP BCIs, the variable $\mathbf{X}$ denotes EEG signals from multiple channels, represented as $\mathbf{X} \in \mathbb{R}^{P \times N_s}$, where P is the number of channels and N_s is the number of samples collected in each channel. The variable $\mathbf{Y} \in \mathbb{R}^{Q \times N_s}$ represents the reference signals, where Q is the number of reference signals. For unsupervised detection of evoked potentials, the reference signals are generated using sine and cosine waves [7]

$$\mathbf{Y}_{f_k} = \begin{bmatrix} \sin(2\pi f_k t) \\ \cos(2\pi f_k t) \\ \vdots \\ \sin(2\pi N_h f_k t) \\ \cos(2\pi N_h f_k t) \end{bmatrix}, \quad t = \frac{1}{f_s}, \frac{2}{f_s}, \ldots, \frac{N_s}{f_s}, \tag{7}$$

with f_k being the fundamental stimulus frequency, f_s is the sampling rate of the signals, and N_h is the number of harmonics considered in the analysis. The total number of signals composing each matrix $\mathbf{Y}_{f_k}$ is given by $Q = 2N_h$.

Based on the canonical correlation coefficients extracted for each reference signal associated with a stimulus presented in the interface, it is possible to construct a classification mechanism that infers the active frequency f_a in a visual stimulation window.

For each stimulation frequency presented in the interface, f_k, the maximized correlation between this frequency and the recorded EEG signals is calculated. Therefore, for each frequency, the projection vectors $\mathbf{z}_{\mathbf{x_k}} \in \mathbb{R}^{Q \times 1}$ and $\mathbf{z}_{\mathbf{y_k}} \in \mathbb{R}^{P \times 1}$ are obtained, which are responsible for generating the linear combinations of the EEG signals and the reference signals, respectively.

The frequency that exhibits the highest correlation coefficient, i.e., the one that produces the largest value ρ_k, is selected as the active frequency. The classification mechanism is described by the following equation [4]

$$f_a = \max_{f_k} \rho_k, \quad k = 1, 2, \ldots, M, \tag{8}$$

where M denotes the total number of visual stimuli used in the interface.

B. Evaluation metrics

To evaluate the performance of the filtering system, classification accuracy and ITR [1] (bits/minute) were employed, as these are metrics widely used in BCI systems [10]. The ITR can be estimated using the following equation

$$ITR = \left(\log_2 M + P\log_2 P + (1-P)\log_2\left(\tfrac{1-P}{M-1}\right)\right) \times \tfrac{60}{T} \tag{9}$$

where P is the classification accuracy, and T (in seconds/selection) is the average time required to make a selection, including both gaze fixation time and the time needed to shift visual focus. In this study, the gaze shift time was set 0.55 s [10]. Thus, this metric represents a good measure of the trade-off between accuracy and classification time.

C. Benchmark Dataset

In this study, the publicly available dataset provided by Tsinghua University was used [10]. The dataset was acquired for a BCI-SSVEP study. The visual interface consisted of 40 visual stimuli, forming a virtual keyboard with 26 English alphabet letters, 10 digits and four non-alphanumeric symbols. The experiment involved 35 healthy participants, all with normal or corrected-to-normal vision. Data collection included EEG recordings from 64 channels, meaning 64 electrodes placed on each participant's scalp. The visual stimuli had frequencies ranging from 8 Hz to 15.8 Hz, with intervals of 0.2 Hz between them. Each stimulation frequency was associated with a specific phase, with a phase difference of 0.5 π between adjacent frequencies. For each participant, six blocks of 40 trials were recorded, with all 40 stimuli indicated by a visual cue in random order. Each trial lasted five seconds. The data sampling rate was 250 Hz.

D. Experimental Setup

The developers of the dataset [10] used the electrode set Pz, PO5, PO3, POz, PO4, PO6, O1, Oz, and O2 to detect evoked potentials. In our analysis, we evaluated the individual performance of each of these electrodes in terms of accuracy and ITR. Based on this evaluation, we selected the top five electrodes: PO3, POz, O1, Oz, and O2. These electrodes were used as the primary signals $d_i(n)$, $i = 1, \ldots, 5$.

To investigate whether electrodes from different cortical regions could be used as reference signals, we defined six sets of non-occipital electrodes, with each set containing $K = 3$

signals. These sets, denoted as C_1 to C_6, were selected from distinct cortical areas:

- C_1 — Pre-frontal: (FP1, FPz, FP2)
- C_2 — Frontal: (F1, Fz, F2)
- C_3 — Frontal-central: (FC1, FCz, FC2)
- C_4 — Central: (C1, Cz, C2)
- C_5 — Central-parietal: (CP1, CPz, CP2)
- C_6 — Parietal: (P1, Pz, P2)

We decided to adopt a fixed configuration of 8 electrodes, considering that low-cost EEG acquisition systems such as the basic version of OpenBCI Cyton [11] support only 8 channels. This constraint ensures that the proposed technique remains applicable in practical scenarios where electrode placement must be more selective and carefully planned.

A Butterworth band-pass filter with a passband from 6 to 70 Hz was first applied to the entire dataset. After that, the entire dataset of a single individual was filtered after initializing the RLS algorithm. The filter coefficients were reset when filtering data from a new user. For both the M-RLS-CCA and RLS-CCA, the forgetting factor was set to 0.99 and and the initial inverse of the autocorrelation matrix was set to $0.01\mathbf{I}$. We are considering a scenario in which the characteristics of the EEG signal vary slowly during stimulation, and the SNR of the evoked potentials is high. To determine the ideal number of taps weights used in the filters for each method, a search was conducted by varying the number of taps applied, with N ranging from 1 to 5.

We have three evaluation scenarios:

1) **CCA method:** The first scenario uses only spatial filtering with CCA, utilizing 8 electrodes, with 5 occipital electrodes selected, along with 3 electrodes from the chosen non-occipital set (C_1 to C_6).
2) **RLS-CCA method:** The second scenario involves filtering the 5 occipital electrodes, using the average of each auxiliary signal set. Afterward, the 5 filtered occipital electrodes are used, applying spatial filtering with the CCA.
3) **M-RLS-CCA method:** The third scenario filters the 5 occipital electrodes and applies each set of auxiliary signals directly to the RLS filter. After that, the 5 filtered occipital electrodes are used, applying spatial filtering with the CCA.

In each of the three scenarios, we used $N_h = 5$ harmonics, as suggested in [4]. Each scenario was evaluated across different data lengths, ranging from 0.25 to 5 seconds, with increments of 0.25 seconds. For better interpretability, we report the number of filter taps that yielded the highest ITR for each electrode configuration analyzed.

V. Results

Figures 4, 5, 6, 7, 8, 9 show the accuracy and ITR curves obtained for different data lengths. The error bars indicate the standard error (SE) [4], [10], calculated based on the average performance of the 35 subjects in the dataset.

It can be inferred from the results that, regardless of the non-occipital cortical region used as the source of the interfering signals, both RLS-CCA and M-RLS-CCA outperform the standard CCA method. The findings suggest that temporal information present in the electrodes located outside the occipital lobe can be leveraged to enhance the SNR of occipital signals. This, in turn, facilitates the subsequent spatial filtering process, which directly contributes to improvements in both the classification accuracy and ITR of the system.

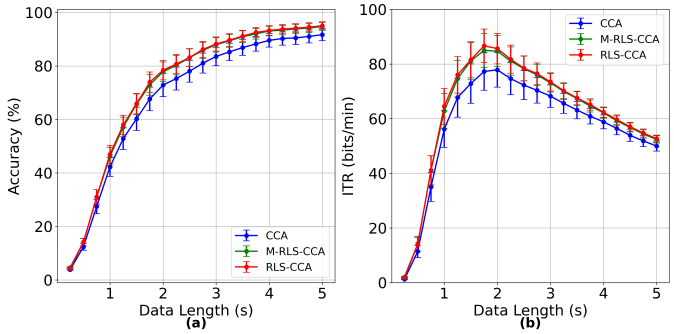

Fig. 4. (a) Classification accuracy. (b) ITRs associated with the accuracy. Reference signals: C_1. Optimal configuration — RLS-CCA: 4 taps; M-RLS-CCA: 2 taps for each reference signal.

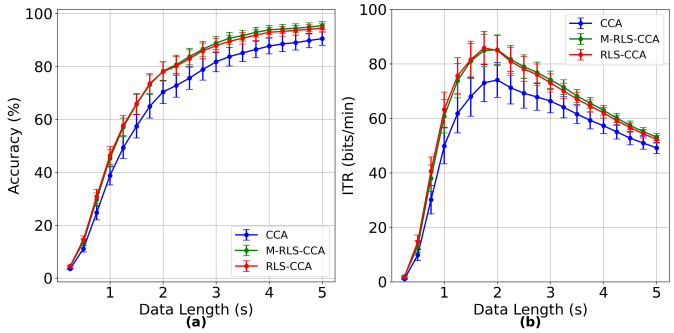

Fig. 5. (a) Classification accuracy. (b) ITRs associated with the accuracy. Reference signals: C_2 Optimal configuration — RLS-CCA: 2 taps; M-RLS-CCA: 3 taps for each reference signal.

Considering the ITR metric, the best configuration obtained using only CCA was with the electrode set C_6, which resulted in a maximum ITR of $81.92 \pm 6.81\%$. For the RLS-CCA technique, the best result was achieved using the C_5 set, reaching $86.78 \pm 6.22\%$. For the method proposed in this work, M-RLS-CCA, the best performance was also obtained

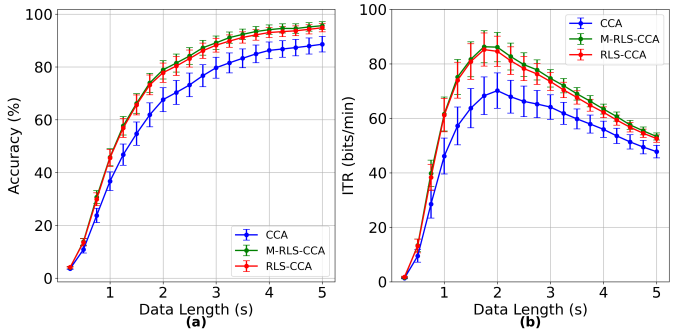

Fig. 6. (a) Classification accuracy. (b) ITRs associated with the accuracy. Reference signals: C_3. Optimal configuration — RLS-CCA: 2 taps; M-RLS-CCA: 2 taps for each reference signal.

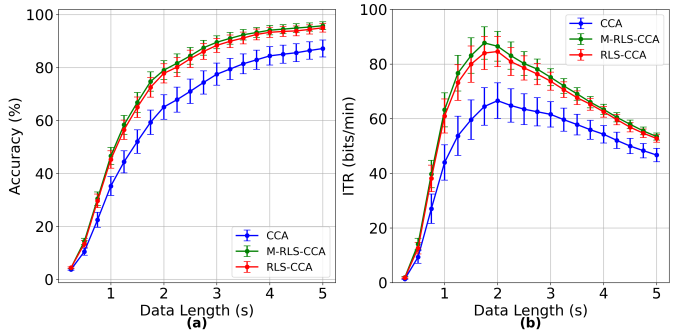

Fig. 7. (a) Classification accuracy. (b) ITRs associated with the accuracy. Reference signals: C_4. Optimal configuration — RLS-CCA: 5 taps; M-RLS-CCA: 1 tap for each reference signal.

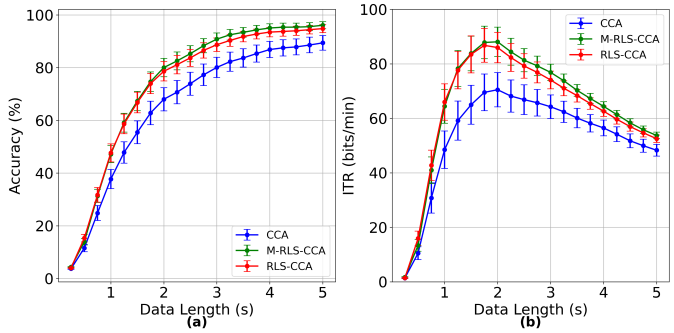

Fig. 8. (a) Classification accuracy. (b) ITRs associated with the accuracy. Reference signals: C_5. Optimal configuration — RLS-CCA: 2 taps; M-RLS-CCA: 2 taps for each reference signal.

using the C_6 set, with a peak ITR of $88.55 \pm 5.99\%$. In all cases, the data length that allowed for maximum information extraction was 1.75 s. The proposed method showed a slight improvement compared to the traditional method. For any set of auxiliary electrodes used, the strategy of averaging the signals or designing a specific filter for each signal yielded very similar results.

Since the goal was to use only 8 electrodes, with only 3 used as reference signals, averaging the interfering signals can be effective, as there may be little variability among the reference signals. Furthermore, each reference electrode set is located in the same region, so the signals captured by these electrodes tend to be highly correlated. A future analysis, considering a larger number of electrodes and combining distinct cortical regions, may generate greater variability in the results obtained by filtering techniques. However, the objective of this work was to verify whether signals from different cortical regions could be used to improve accuracy and ITR compared to the exclusive application of CCA. It can be affirmed that they can, since, in all sets from C_1 to C_6, the performance of the purely spatial filtering using CCA was inferior to the RLS-CCA and M-RLS-CCA.

VI. Conclusions

In this paper, we propose the M-RLS-CCA algorithm to mitigate interference in EEG signals in the context of an SSVEP BCI. The numerical results obtained show that the proposed method exhibits a slight improvement in performance

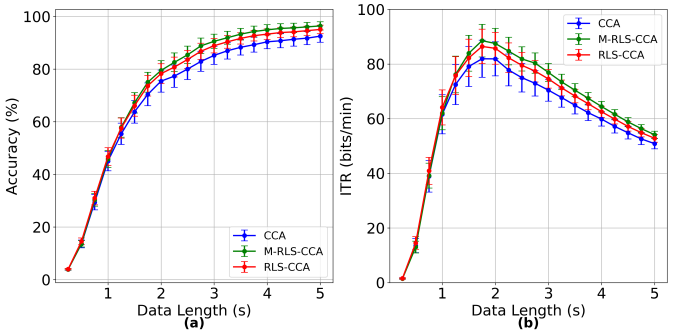

Fig. 9. (a) Classification accuracy. (b) ITRs associated with the accuracy. Reference signals: C_6. Optimal configuration — RLS-CCA: 4 taps; M-RLS-CCA: 2 taps for each reference signal.

compared to the original RLS-CCA method. For the proposed algorithm, the set C_6 produced the best results, using 2 taps for each reference signal. In the case of RLS-CCA, the best performance was achieved with set C_5, also using a filter with only 2 taps. This indicates that the filtering systems do not require many parameters to achieve optimal performance. The experimental results also showed an advantage in applying temporal filtering before spatial filtering using CCA. Moreover, the results demonstrated that for any non-occipital region selected, it was possible to achieve better outcomes than only using spatial filtering. In future work, we intend to increase the number of channels used to mitigate interference. This will help verify whether averaging the filtered reference signals still yields comparable results, especially when the reference signals come from different non-occipital regions.

References

[1] J. R. Wolpaw, N. Birbaumer, D. J. McFarland, G. Pfurtscheller, and T. M. Vaughan, “Brain–computer interfaces for communication and control,” *Clinical Neurophysiology*, vol. 113, no. 6, pp. 767–791, 2002.

[2] S. N. Carvalho, T. B. S. Costa, L. F. S. Uribe, D. C. Soriano, G. F. G. Yared, L. C. Coradine, and R. Attux, “Comparative analysis of strategies for feature extraction and classification in SSVEP BCIs,” *Biomedical Signal Processing and Control*, vol. 21, pp. 34–42, 2015.

[3] R. Abiri, S. Borhani, E. W. Sellers, Y. Jiang, and X. Zhao, “A comprehensive review of EEG-based brain–computer interface paradigms,” *Journal of Neural Engineering*, vol. 16, no. 1, p. 011001, 2019.

[4] X. Chen, Y. Wang, S. Gao, T.-P. Jung, and X. Gao, “Filter bank canonical correlation analysis for implementing a high-speed SSVEP-based brain–computer interface,” *Journal of Neural Engineering*, vol. 12, no. 4, p. 046008, 2015.

[5] D. Regan, "Human brain electrophysiology", *Evoked Potentials and Evoked Magnetic Fields in Science and Medicine*, Elsevier, 1989.

[6] J. Castillo, S. Müller, E. Caicedo, and T. Bastos, “Feature extraction techniques based on power spectrum for a SSVEP-BCI,” in *Proceedings of the 2014 IEEE 23rd International Symposium on Industrial Electronics (ISIE)*, 2014, pp. 1051–1055.

[7] Z. Lin, C. Zhang, W. Wu, and X. Gao, “Frequency recognition based on canonical correlation analysis for SSVEP-based BCIs,” *IEEE Transactions on Biomedical Engineering*, vol. 54, no. 6, pp. 1172–1176, 2007.

[8] S. Wang, B. Ji, D. Shao, W. Chen, and K. Gao, “A methodology for enhancing SSVEP features using adaptive filtering based on the spatial distribution of EEG signals,” *Micromachines*, vol. 14, no. 5, p. 976, 2023.

[9] S. Haykin, "Adaptive Filter Theory, 4th ed., Prentice Hall, 2001.

[10] Y. Wang, X. Chen, X. Gao, and S. Gao, “A benchmark dataset for SSVEP-based brain–computer interfaces,” *IEEE Transactions on Neural Systems and Rehabilitation Engineering*, vol. 25, no. 10, pp. 1746–1752, 2016.

[11] OpenBCI. *OpenBCI: Open Source Biosensing Tools*. Available at: https://openbci.com/. Accessed: May 8, 2025.